MgN: A possible material for spintronic applications

A. Droghetti, N. Baadji, and S. Sanvito
School of Physics and CRANN, Trinity College, Dublin 2, Ireland

(Received 29 June 2009; revised manuscript received 22 September 2009; published 8 December 2009)

We present rocksalt MgN as a d^0 magnet with potential for spintronics applications. Our density-functional theory calculations demonstrate that rocksalt MgN is at the verge of half-metallicity, with an electronic structure robust against the choice of exchange and correlation functional. Furthermore the calculated heat of formation describes the compound as metastable and suggests that it can be fabricated by tuning the relative Mg and N abundance during growth. Intriguingly the equilibrium lattice constant is close to that of MgO so that MgN is likely to form as an inclusion during the fabrication of N-doped MgO. If MgN can be made, the MgO/MgN system may become a materials platform for magnetic tunnel junctions not incorporating any transition metals.

DOI: 10.1103/PhysRevB.80.235310 PACS number(s): 75.50.Cc, 71.20.Ps

I. INTRODUCTION

The so-called d^0 magnets are challenging our conventional understanding of magnetism. These are wide-gap semiconductors and oxide insulators displaying magnetic properties which cannot be ascribed to the presence of partially filled d or f shells.[1] Prototypical examples are diamagnetic materials in their well crystallized bulk form, which present magnetic features when grown as defective thin films. A similar phenomenology is found also in oxides doped with light elements such as N or C.[2,3] Unfortunately, despite the increasingly large number of reports of d^0 magnets, their typical experimental characterization is often limited to magnetometry with little information about the local electronic structure. The phenomenon thus remains rather obscure. It is characterized by a poor degree of reproducibility and still lacks of a convincing theoretical framework.

Most of the theoretical work to date is based on density-functional theory (DFT) utilizing local approximations to the exchange and correlation functional (LDA or GGA). In most of the cases the LDA/GGA, probably correctly, associates the magnetic-moment formation to spin-polarized holes residing on either cation vacancies or impurities. In addition the ground state is always predicted ferromagnetic and rather robust. However LDA and GGA usually fail in describing the symmetry details of the wave function, in particular the polaronic distortion around the magnetic center. This essentially originates since LDA and GGA tend to delocalize the charge density in order to minimize the spurious self-interaction.[4] Therefore more advanced techniques, including self-interaction corrections at least in an approximate way, appear as necessary.[5–9] When applied, these confirm the nature of the magnetic-moment formation but almost always predict no long-range magnetic coupling and no ferromagnetism. MgO:N is a prototypical example.[5,6,10,11] Quantum Monte Carlo calculations for the Anderson-Haldane model indicates the possibility of high-temperature ferromagnetism.[11] However DFT calculations using either the LDA+U or the self-interaction correction (SIC) scheme return impurity levels deep in the gap, holes trapped by polaronic distortions and no room-temperature ferromagnetism.[5,6,10]

Finally another important, but yet scarcely studied, class of d^0 magnets is represented by zinc-blende (ZB) II-V or II-IV compounds such as CaP, CaAs, CaSb (Refs. 12–14) or CaC, SrC, and BaC.[15] These are weakly covalent solids with either one or two holes per formula unit, and they are generally predicted to be half-metallic. Intriguingly, although at least for the II-V's the thermodynamical stable phase has the stoichiometric Zn_3P_2-type structure,[16] their rock-salt (RS) phase has usually a lower energy than the ZB and it is predicted metastable.

In this work we investigate the magnetic ground state of RS MgN, which was already predicted as half-metal in the ZB phase.[14] This is an extremely interesting material because of its structural similarity to the parental MgO, widely used as tunnel barrier in magnetic tunnel junctions.[17] We will demonstrate that RS MgN is a half-metal with negligible spin-orbit interaction and negative formation enthalpy. Therefore we conclude that, although the RS may not be the thermodynamical stable phase and the off stechiometric nature of the compound does not allow for the formation of bulk samples, RS MgN might still be grown as a metastable phase. In particular we speculate that either very thin films (just a few layers) grown on a suitable substrate or small nanoclusters inside MgO matrices can be made.

II. COMPUTATIONAL METHOD

Our calculations are performed with a development version of the SIESTA code,[18] which includes the atomic self-interaction correction (ASIC) (Ref. 19) and the LDA+U (Ref. 20) schemes. The core electrons are treated with norm-conserving Troullier-Martin pseudopotentials and the valence charge density is expanded over a numerical orbital basis set, including double-ζ and polarized functions.[18] The real-space grid has an equivalent cutoff larger than 600 Ry, and we sample a minimum of $20\times20\times20$ k points in the Brillouin zone. The atomic coordinates are relaxed by conjugate gradient until the forces are smaller than 0.01 eV/Å. For the evaluation of the spin-orbit coupling we have performed full-potential linear augmented plane-wave (FLAPW) calculations[21] with the scheme implemented in FLEUR code.[22] We use a $12\times12\times12$ k-point mesh and a

TABLE I. Equilibrium lattice constant a (in Å), magnetic moment per formula unit μ (in μ_B) and ΔE_M (in meV) for ZB and RS MgN.

	LDA			GGA		
Structure	a	μ	ΔE_M	a	μ	ΔE_M
ZB	4.73	1.0	157	4.83	1.0	180
RS	4.34	1.0	60	4.44	1.0	95

plane-wave expansion with $k_{max}=4$ a.u. A muffin-tin sphere of a radius 2.02 Bohr was taken for both Mg and N with $\ell_{max}=8$ as cutoff in the ℓ expansion of the muffin orbitals. Spin orbit is included by second variation method.[23]

III. RESULTS AND DISCUSSION

A. Electronic structure

We start our analysis by briefly comparing the ground state of the ZB and RS structures. In Table I we report the equilibrium lattice constant, a, the magnetic moment per formula unit, μ, and the magnetic-moment formation energy, ΔE_M, for the two structures. ΔE_M is defined as the energy difference per formula unit between the spin-polarized and the nonspin-polarized DFT solution and it is positive when the magnetic state has a lower energy. Importantly ΔE_M is always substantially larger than zero, demonstrating that the magnetism is robust for both the structures. We also note that our results for the ZB phase are in excellent agreement with previous calculations[14] and that for the RS phase ΔE_M is slightly smaller than that calculated for the same phase of SrN and CaN.[16]

Next we discuss in details the electronic structure of RS MgN. The GGA band structure calculated at the equilibrium lattice constant of 4.44 Å and displayed in Fig. 1, clearly reveals the half-metallic character of MgN with a direct gap of 5 eV at the Γ point in the majority spin channel. This is

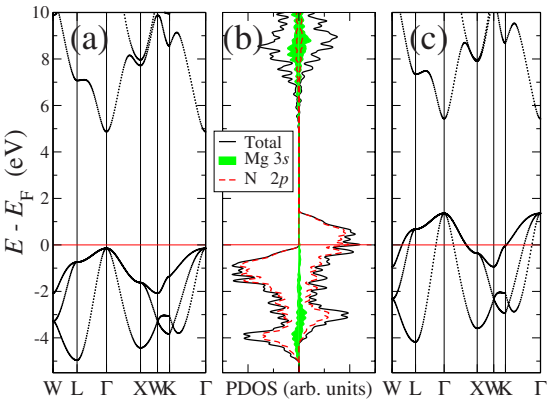

FIG. 1. (Color online) GGA band structure for RS MgN calculated at the equilibrium lattice constant of 4.44 Å: panel (a) majority spin, panel (c) minority. The horizontal red line denotes the position of Fermi level. In panel (b) we report the associated total density of states (black solid line) and density of states projected over the N-2p (red dashed line) and Mg-3s (green shadowed area).

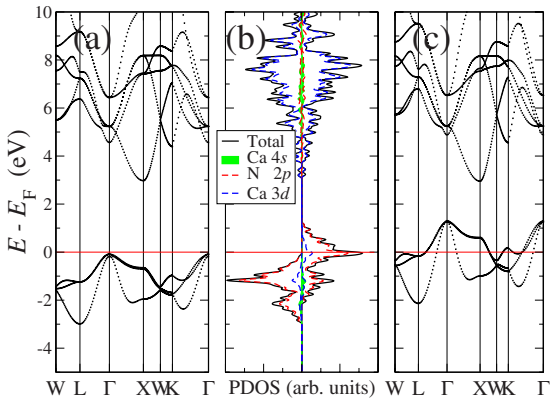

FIG. 2. (Color online) GGA band structure for RS CaN calculated at the equilibrium lattice constant of 5.0 Å: panel (a) majority spin, panel (c) minority. The horizontal red line denotes the position of Fermi level. In panel (b) we report the associated total density of states (black solid line) and density of states projected over the N-2p (red dashed line), Ca-4s (green shadowed area), and Ca-3d (blue dashed line).

different from the bandstructure for RS CaN where the gap is indirect with the conduction-band minimum located at X.[16]

The differences between CaN and MgN can be understood by looking at the orbital projected density of states (PDOS) presented in Fig. 1(b) for MgN and in Fig. 2(b) for CaN. In the case of MgN the N 3d levels are unbound and they only weakly mix with the Mg 3s, which form the conduction band. In contrast the empty Ca 3d levels provide the dominant contribution to the conduction band of CaN, shifting the band minimum to the X point. Furthermore their hybridization with the N 2p orbitals forming the valence band is rather strong and result in the CaN valence band being considerably more flat than that of MgN. In summary the main difference between RS MgN and CaN is in the different role played by the cation 3d orbitals. Interestingly it was suggested[12] that the contribution of the Ca-d level in Ca pnictides is fundamental to promote the half-metallicity. Later such a claimed was challenged by the statement that the magnetic-moment formation in II-V compounds is driven by the strong atomic character of the anions.[16] MgN demonstrates that both of the arguments are partially correct. Indeed the ionicity in SrN, CaN, and MgN is able to localize the hole on N leading to the formation of the magnetic moment. However the hybridization with the d shell of the cation increases the flatness of the top of valence band causing an enhancement of ΔE_M.

We then investigate the robustness of the half-metallic ground state with respect to compression. In Fig. 3 we report the magnetic moment as a function of the lattice constant as calculated with GGA (the LDA results are rather similar). Importantly we note that there is a broad range of lattice constants for which MgN preserves the half-metal moment of 1 μ_B. For a smaller than 4.3 Å the moment becomes fractional and the material turns into a standard magnetic metal, until it finally becomes nonspin polarized for a massive compressive pressure ($a<3.0$ Å). Interestingly at the MgO lattice constant (4.21 Å) the magnetic state of MgN is still extremely close to that of a half-metal. This is a tanta-

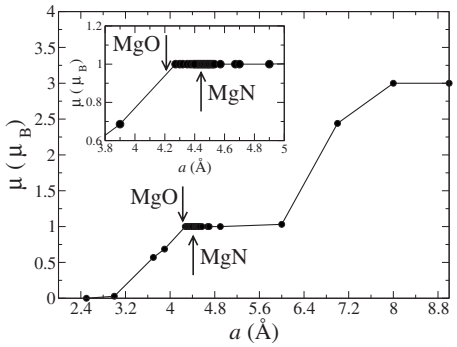

FIG. 3. Magnetic moment μ per formula unit as a function of the lattice constant for RS MgN as calculated with GGA. The inset shows a zoom at around the GGA equilibrium value of 4.44 Å. The arrows indicate the experimental MgO and the GGA-calculated MgN lattice constants.

lizing feature suggesting that, should MgN be made in MgO, it will be an efficient spin polarizer/analyzer in transition-metal free tunnel junctions. Finally note that for a largely expanded lattice parameter the moment reaches the value of 3 μ_B expected from isolated N ions.

B. Magnetism

Magnetic properties and the possible effects arising from on-site Coulomb repulsion are analyzed next. We start by estimating the critical temperature for the moment formation. This can be simply calculated from the Stoner criterion adapted to spin-polarized density-functional theory[24] by finding the temperature, T_M, that satisfies the equation

$$I(E_F)\int_{-\infty}^{\infty}\frac{\partial f(E)}{\partial E}N(E)dE + 1 = 0 \quad (1)$$

where $N(E)$ is the density of states,

$$f(E) = \frac{1}{1+\exp[(E-\mu)/kT]} \quad (2)$$

is the Fermi function, and k is the Boltzmann constant. $I(E_F)$ is the generalized Stoner parameter evaluated from the band spin splitting measured with respect to the nonmagnetic solution and with the assumption not to depend on the lattice wave vector. We find the remarkably large value of T_M=20 000 K. Although this might appear as an unrealistically high temperature, we have to remind that T_M does not coincide with the Curie temperature, which is often determined mainly by the transverse spin fluctuations (i.e. spin waves) rather than the longitudinal ones. In fact T_M is predicted to be about a few thousand kelvin for every ferromagnetic transition metal.[24] Interestingly, T_M for MgN is considerably larger than that of bcc Fe. This result points once again to the uniqueness of p-type magnetism. In fact the exchange interaction in the p shell is calculated to be up to three times larger than that in the d.[25] No magnetism is usually found for p electrons because of the typical small DOS associated to the saturated bonds. However this is not the case in MgN where the $N(E_F)$ is large due to the favorable stoichiometry and the flatness of the valence band. Thus the p-derived DOS in MgN is comparable to that of the d shell of Fe, but the exchange is much larger, resulting in a larger Stoner temperature T_M.

TABLE II. Critical lattice constant for the half-metallicity, a_c, minority-spin band gap, E_{gap}, exchange split ΔE_{ex}, and ferromagnetic to antiferromagnetic total-energy difference $\Delta E^{I}_{\uparrow\uparrow-\uparrow\downarrow}$ and $\Delta E^{II}_{\uparrow\uparrow-\uparrow\downarrow}$, as a function of the on-site Coulomb interaction U.

U (eV)	a_c (Å)	E_{gap} (eV)	ΔE_{ex} (eV)	$\Delta E^{I}_{\uparrow\uparrow-\uparrow\downarrow}$ (meV)	$\Delta E^{II}_{\uparrow\uparrow-\uparrow\downarrow}$ (meV)
GGA	4.3	5.0	1.51	52	53
2	3.8	6.19	2.15	95	96
3	3.6	6.40	2.48	172	156
4	3.5	6.75	2.94	267	251
5	3.4	7.16	3.30	344	338
6	3.4	7.40	3.77	395	392
7	3.3	8.09	4.23	443	428
8	3.2	8.17	4.68	472	463
ASIC	3.6	7.51	4.24	184	175

Next we investigate the robustness of the ferromagnetic state against possible antiferromagnetic configurations. In particular we calculate the total-energy difference per formula unit between the ferromagnetic and either the type-I ($\Delta E^{I}_{\uparrow\uparrow-\uparrow\downarrow}$) and type-II ($\Delta E^{II}_{\uparrow\uparrow-\uparrow\downarrow}$) antiferromagnetic states. These are both characterized by a planar ferromagnetic alignment with antiparallel orientation between planes, either along the (001) (type-I) or (111) (type-II) direction. Certainly many other antiferromagnetic configurations can be investigated, however type I and type II are the most recurrent in RS magnets, so that they are expected to be the most relevant here. At the equilibrium lattice constant we find $\Delta E^{I}_{\uparrow\uparrow-\uparrow\downarrow}$=52 meV ($\Delta E^{I}_{\uparrow\uparrow-\uparrow\downarrow}$=67 meV) and for $\Delta E^{II}_{\uparrow\uparrow-\uparrow\downarrow}$=53 meV ($\Delta E^{II}_{\uparrow\uparrow-\uparrow\downarrow}$=68 meV) for LDA (GGA). These value, when mapped onto a second-nearest-neighbor Heisenberg model, give ferromagnetic exchange constants and a mean-field Curie temperature, T_C, of 592 K. Although it is well know that the mean-field approximation usually overestimates T_C, this result clearly suggests that MgN could be ferromagnetic well above room temperature. Comparing T_M and T_C we can also notice that, as in standard transition metals, the magnetic moments survive well above the ferromagnetic to paramagnetic transition.

It is then interesting to investigate how the moment formation depends on electron localization. This is studied using the LDA+U scheme applied to the N-2p shell as a function of U (J is kept at zero). Our results are reported in Table II. As expected LDA+U shifts down the N-2p shell center of mass effectively opening the band gap in both the spin bands. This is associated to a considerable strengthening of the ferromagnetic interaction, with both $\Delta E^{I}_{\uparrow\uparrow-\uparrow\downarrow}$ and $\Delta E^{II}_{\uparrow\uparrow-\uparrow\downarrow}$ increasing monotonically with U. In Table II we also report the exchange split, ΔE_{ex}, which is the energy difference between the top of the majority and minority valence bands for the ferromagnetic ground state at its equilibrium lattice constant. We note that also Δ_{ex} increases with U with an almost

perfectly linear dependence. Finally we find that the critical lattice constant for the half-metallicity gets progressively reduced as U gets larger, while the equilibrium lattice parameter seems to be only marginally affected by U.

The promotion of the magnetic stability in RS MgN with increasing U can be understood by using the DFT version of the standard Stoner argument applied to the LDA+U functional.[24–26] In fact, in the limit of uniform occupancy of the strongly correlated shell (N-2p in our case), one expects the Stoner parameter to increase linearly with U. This may, of course, be compensated by a reduction of the density of states at the Fermi energy (E_F), resulting in an overall reduction of the magnetic interaction. In the case of RS MgN, however, both the bandwidth and the curvature of the bands near E_F change little with U, since such a valence band has a pure N-2p character. As a consequence we find an almost perfect linear relation between the exchange split ΔE_{ex} and U, which confirms the itinerant nature of the ferromagnetism in MgN. This leads us to conclude that the addition of on-site Coulomb repulsion enhances the stability of the half-metal character of RS MgN.

In Table II we also report results obtained with the ASIC method, which was proved to yield an accurate MgO band-gap and the proper polaronic distortion in diluted d^0 magnets.[5] The ASIC returns both a critical lattice constant for the half-metallicity and magnetic energies similar to those calculated with LDA+U and $U \sim 3$ eV. However the band gap and Δ_{ex} are considerably larger and compatible with $U=6$ eV. Although it is difficult to make any strong quantitative statement, because the mixed success of ASIC in predicting exchange constants,[27] the result further confirms that the half-metallic state of MgN is strong with respect to on-site Coulomb repulsion.

Finally we investigate the effect of the spin-orbit coupling on the electronic structure of MgN. In general spin-orbit interaction always destroys the half-metallicity of a magnet by mixing the two spin channels. Our calculations however show that the spin-orbit coupling constant between the spin and the orbital angular momentum is only of the order of 10 meV. Furthermore, the MgN highly symmetric cubic environment quenches the angular magnetic moment, which is only $7\times10^{-5}\mu_B$ for Mg and $9.8\times10^{-4}\mu_B$ for N. It is then not surprising that the spin polarization remains 100% even after the spin-orbit interaction is accounted for; i.e., the half-metallicity is preserved.

C. Structural and thermodynamical properties

After having discussed the electronic properties of MgN we now turn our attention to analyzing the structural stability of the RS structure. First we compare the total energy per cell of volume of five different crystal structures, likely candidates for MgN, namely, wurzite, ZB, NiAs-type (space group $P6_3/mmc$), RS and hexagonal MgO (h-MgO). The last one is obtained from the wurtzite by moving the cations towards the anion plane, so that the coordination increases from 4 to 5. This is a phase often encountered in semiconductors with zincblende/wurtzite structure under pressure along the phase transformation to the RS phase.[28,29] Moreover it is also a likely intermediate phase of CoO in the spontaneous transition from wurtzite to RS.[20] Importantly such a phase has always a volume lower than that of the zincblende/wurtzite structure so that it might appear as a serious competitor of RS when the volume is forced to be small, for instance when the materials is grown as inclusion within a host with smaller lattice parameters.

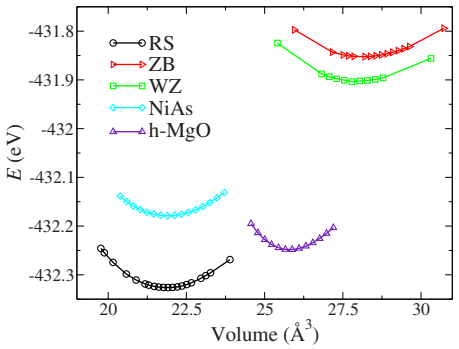

FIG. 4. (Color online) Total energy as a function of the volume per formula unit for MgN with wurtzite (WZ), zincblende (ZB), NiAs, rock-salt (RS), and hexagonal-MgO (h-MgO) crystal structures.

As shown in Fig. 4 the RS structure presents both the lower total energy and smaller equilibrium volume of all the crystals investigated, indicating that it is the most thermodynamic favorable. We further confirmed this result by distorting the RS structure either orthorhombically and tetrahedrally and by proving that such distortions indeed increase the total energy. Although a conclusive argument can only be obtained by calculating the entire phonon spectrum in the search for unstable modes, our results strongly suggest that the RS is probably the lowest energy structure in the Mg-N phase diagram for the one to one stechiometry. This however still does not mean that MgN can be made. In fact one has to compare the stability of RS MgN with that of its stechiometric stable form Mg_3N_2, i.e. one has to demonstrate that the heat of formation for RS MgN, ΔH_{MgN}, is comparable to that of Mg_3N_2, $\Delta H_{Mg_3N_2}$.

Mg_3N_2 is a nonmagnetic semiconductor with an experimental band gap of 2.8 eV (Ref. 31) and with the tetragonal bixbyite crystal structure. The experimental lattice constant is 9.953 Å (Ref. 30) while our calculations return values of 9.85 (LDA) and 10.01 Å (GGA). These are both within 1% of the experimental reported values. The heats of formation can be written as

$$\Delta H_{Mg_3N_2} = E_{Mg_3N_2} - 3E_{Mg} - E_{N_2}, \tag{3}$$

$$\Delta H_{MgN} = E_{MgN} - E_{Mg} - \frac{1}{2}E_{N_2}, \tag{4}$$

where E is the elementary reference energy per atom and Mg is assumed in its hcp metallic phase. We calculate $\Delta H_{Mg_3N_2}=-7.2$ eV($\Delta H_{Mg_3N_2}=-5.8$ eV) and $\Delta H_{MgN}=-1.82$ eV($\Delta H_{MgN}=-1.18$ eV) with LDA (GGA). Although, as expected Mg_3N_2 has a lower heat of formation and forms at equilibrium, RS MgN also has a negative ΔH.

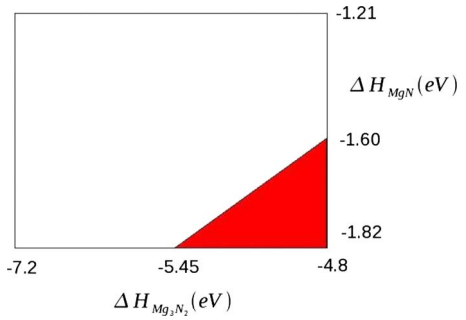

FIG. 5. (Color online) Schematic representation of the regions of stability for the MgN and Mg_3N_2 phases under N-rich conditions. Along the axes we report $\Delta H_{Mg_3N_2}$ and ΔH_{MgN} within 20 % from the calculated LDA values. The regions colored in red (white) are those where MgN (Mg_3N_2) is thermodinamically more stable.

This means that it is a thermodynamic stable compound, and hence that RS MgN is at least metastable. We then further investigate whether or not the relative abundance of N and Mg during the growth process can drive the formation of MgN over that of Mg_3N_2. Then we have to calculate for which values of the N and Mg chemical potential (indicated respectively with $\Delta\mu_N$ and $\Delta\mu_{Mg}$) the stability condition[32]

$$\Delta\mu_N + \Delta\mu_{Mg} = \Delta H_{MgN}, \tag{5}$$

is satisfied with the constrain

$$2\Delta\mu_N + 3\Delta\mu_{Mg} \leq \Delta H_{Mg_3N_2}. \tag{6}$$

However it is important to point out that such a procedure is not free of uncertainty, since the typical DFT error in evaluating the enthalpies of formation can be as large as 1 eV per cell. Thus, in order to obtain quantitative predictions one has to include corrections, that require an extensive fit to known experimental results.[32] Unfortunately there are no experimental data available for the MgN stechiometry. Hence we took a more pragmatic approach and we evaluate the enthalpy of formation for N-rich conditions assuming a possible overestimation of the order of 20%, which is the error for Mg_3N_2 estimated by comparing our results with previous calculations and experimental data.[32]

The mapping of Fig. 5 graphically illustrates the regions of stability of MgN and Mg_3N_2 as calculated with LDA. Along the axes we list the values of $\Delta H_{Mg_3N_2}$ and ΔH_{MgN} within 20% from the calculated DFT values. We then color in red regions where, under N-rich conditions, MgN forms over Mg_3N_2 and in white regions where the opposite happens. We note that, although for values of $\Delta H_{Mg_3N_2}$ and ΔH_{MgN} as calculated from LDA, MgN never seems to form, this is no longer true when the experimental value for $\Delta H_{Mg_3N_2}$, which is equal to −4.8 eV,[32] is considered. Indeed, in this case, MgN is predicted stable for a wide range of values of ΔH_{MgN} within the chosen interval. Otherwise, according to the GGA calculations, MgN never seems to form.

Unfortunately we cannot set a more stringent limit for the formation of RS MgN and we wish to remark that the growth over a particular substrate or as an inclusion in a host and in out-of-equilibrium conditions can partially invalidate the rigorous thermodynamical arguments. This is the case for instance of zincblende MnAs, which is unfavorable to the growth in the bulk due to the competition with the NiAs-type structure,[33] but it was grown in the form of tiny dots in GaAs.[34] We then believe that, although MgN is unlikely to form as a bulk crystal because of its nonstechiometic nature, our results still suggest that it might be grown as small nanoclusters inside MgO. Furthermore few layers of MgN could also be grown on an suitable substrate. In addiction to MgO, metals with bcc lattice structure are for instance equally tantalizing substrates. Among them we mention V, Mo, and W.

IV. CONCLUSIONS

In conclusion we have demonstrated that rocksalt MgN is a d^0 magnet at the verge of half-metallicity, and that the half-metallic ground is robust with respect to both compression and spin-orbit interaction, and it is strengthened by an additional on-site potential introduced through the LDA+U or the ASIC method. Furthermore we have shown that the RS phase is the most stable among the various possible MgN phases. Its heat of formation is negative, but smaller than that of Mg_3N_2, suggesting that MgN can be possibly made by tuning the relative Mg and N abundances during growth and the substrate crystal structure. If made, MgN, together with MgO, can become an ideal materials platform for d^0 tunnel junctions.

ACKNOWLEDGMENTS

This work is sponsored by Science Foundation of Ireland (Grant No. 07/RFP/MASF238), by the EU Sixth Framework (SpiDME project), and by CRANN. Computational resources have been provided by the HEA IITAC project managed by the Trinity Center for High Performance Computing and by ICHEC.

[1] J. M. D. Coey, Solid State Sci. **7**, 660 (2005).
[2] H. Pan, J. B. Yi, L. Shen, R. Q. Wu, J. H. Yang, J. Y. Lin, Y. P. Feng, J. Ding, L. H. Van, and J. H. Yin, Phys. Rev. Lett. **99**, 127201 (2007).
[3] S. Zhou, Q. Xu, K. Potzger, G. Talut, R. Grötzschel, J. Fassbender, M. Vinnichenko, J. Grenzer, M. Helm, H. Hochmuth, M. Lorenz, M. Grundmann, and H. Schmidt, Appl. Phys. Lett. **93**, 232507 (2008).
[4] J. P. Perdew and A. Zunger, Phys. Rev. B **23**, 5048 (1981).
[5] A. Droghetti, C. D. Pemmaraju, and S. Sanvito, Phys. Rev. B **78**, 140404(R) (2008).
[6] V. Pardo and W. E. Pickett, Phys. Rev. B **78**, 134427 (2008).
[7] I. S. Elfimov, A. Rusydi, S. I. Csiszar, Z. Hu, H. H. Hsieh, H. J. Lin, C. T. Chen, R. Liang, and G. A. Sawatzky, Phys. Rev. Lett.

98, 137202 (2007).
[8] J. A. Chan, S. Lany, and A. Zunger, Phys. Rev. Lett. **103**, 016404 (2009).
[9] S. Lany and A. Zunger, Phys. Rev. B **80**, 085202 (2009).
[10] A. Droghetti and S. Sanvito, Appl. Phys. Lett. **94**, 252505 (2009).
[11] B. Gu, N. Bulut, T. Ziman, and S. Maekawa, Phys. Rev. B **79**, 024407 (2009).
[12] K. Kusakabe, M. Geshi, H. Tsukamoto, and N. Suzuki, J. Phys.: Condens. Matter **16**, S5639 (2004).
[13] O. Volnianska, P. Jakubas, and P. Bogusławski, J. Alloys Compd. **423**, 191 (2006).
[14] M. Sieberer, J. Redinger, S. Khmelevskyi, and P. Mohn, Phys. Rev. B **73**, 024404 (2006).
[15] G. Y. Gao, K. L. Yao, E. Sasioglu, L. M. Sandratskii, Z. L. Liu, and J. L. Jiang, Phys. Rev. B **75**, 174442 (2007).
[16] O. Volnianska and P. Bogusławski, Phys. Rev. B **75**, 224418 (2007).
[17] Stuart S. P. Parkin, Christian Kaiser, Alex Panchula, Philip M. Rice, Brian Hughes, Mahesh Samant, and See-Hun Yang, Nature Mater. **3**, 862 (2004).
[18] J. M. Soler, E. Artacho, J. D. Gale, A. García, J. Junquera, P. Ordejón, and D. Sánchez-Portal, J. Phys.: Condens. Matter **14**, 2745 (2002).
[19] C. D. Pemmaraju, T. Archer, D. Sanchez-Portal, and S. Sanvito, Phys. Rev. B **75**, 045101 (2007).
[20] T. Archer, R. Hanafin, and S. Sanvito, Phys. Rev. B **78**, 014431 (2008).
[21] M. Weinert, E. Wimmer, and A. J. Freeman, Phys. Rev. B **26**, 4571 (1982).
[22] http://www.flapw.de
[23] C. Li, A. J. Freeman, H. J. F. Jansen, and C. L. Fu, Phys. Rev. B **42**, 5433 (1990).
[24] O. Gunnarsson, J. Phys. F: Met. Phys. **6**, 587 (1976).
[25] J. F. Janak, Phys. Rev. B **16**, 255 (1977).
[26] A. G. Petukhov, I. I. Mazin, L. Chioncel, and A. I. Lichtenstein, Phys. Rev. B **67**, 153106 (2003).
[27] A. Akande and S. Sanvito, J. Chem. Phys. **127**, 034112 (2007).
[28] S. Limpijumnong and W. R. L. Lambrecht, Phys. Rev. B **63**, 104103 (2001).
[29] M. Grünwald, E. Rabani, and C. Dellago, Phys. Rev. Lett. **96**, 255701 (2006).
[30] D. E. Partin, D. J. Williams, and M. O'Keeffe, J. Solid State Chem. **132**, 56 (1997).
[31] C. M. Fang, R. A. de Groot, R. J. Bruls, H. T. Hintzen, and G. de With, J. Phys.: Condens. Matter **11**, 4833 (1999).
[32] S. Lany, Phys. Rev. B **78**, 245207 (2008).
[33] S. Sanvito and N. A. Hill, Phys. Rev. B **62**, 15553 (2000).
[34] K. Ono, J. Okabayashi, M. Mizuguchi, M. Oshima, A. Fujimori, and H. Akinaga, J. Appl. Phys. **91**, 8088 (2002).